

Article

# Synergistic Effect of Ag and ZnO Nanoparticles on Polypyrrole-Incorporated Epoxy/2pack Coatings and Their Corrosion Performances in Chloride Solutions

Ubair Abdus Samad <sup>1</sup>, Mohammad Asif Alam <sup>1</sup>, El-Sayed M. Sherif <sup>1,2,\*</sup> , Manawwar Alam <sup>3</sup> , Hamid Shaikh <sup>4</sup> , Nabeel H. Alharthi <sup>1</sup> and Saeed M. Al-Zahrani <sup>4</sup> 

<sup>1</sup> Center of Excellence in Engineering Materials, King Saud University, P.O. Box 800, Riyadh 11421, Saudi Arabia; uabdussamad@ksu.edu.sa (U.A.S.); moalam@ksu.edu.sa (M.A.A.); Alharthi@ksu.edu.sa (N.H.A.)

<sup>2</sup> Electrochemistry and Corrosion Laboratory, Department of Physical Chemistry, National Research Centre, El-Buhouth St., Dokki, Cairo 12622, Egypt

<sup>3</sup> Department of Chemistry, College of Science, King Saud University, P.O. Box 2455, Riyadh 11421, Saudi Arabia; malamiitd@gmail.com

<sup>4</sup> SABIC Polymer Research Center (SPRC), Chemical Engineering Department, King Saud University, P.O. Box 800, Riyadh 11421, Saudi Arabia; hamshaikh@ksu.edu.sa (H.S.); szahrani@ksu.edu.sa (S.M.A.-Z.)

\* Correspondence: esherif@ksu.edu.sa

Received: 13 March 2019; Accepted: 23 April 2019; Published: 26 April 2019



**Abstract:** In this study, two formulae (F1 and F2) of epoxy/2pack coatings incorporated with polypyrrole (PPy)-conducting polymer were produced from bisphenol-A type of epoxy resin (DGEBA) with the addition of Ag and ZnO nanoparticles. The synergism effect of Ag and ZnO nanoparticles on the mechanical and corrosion resistance properties was reported. The curing agent 2,4,6-tris(dimethylaminomethyl) phenol (ARADUR 3282-BD) was used under optimized stoichiometry values. The nanoparticles ratio in different wt.% were first dispersed in solvent by the sonication process and then added to epoxy/PPy composition. All the coated steel panels were cured at room temperature in a controlled dust free environment for 7 days in order to obtain a hard and intact coating. The dispersion of nano-size ZnO and Ag pigments was investigated using scanning electron microscopy (SEM) and its composition through an energy dispersive X-ray (EDX) technique. Conventional techniques and nano-indentation were also performed to observe the effect of ZnO and Ag synergism content on the hardness and modulus of elasticity at nano scale. The corrosion behavior of the coated samples was investigated at room temperature in 3.5% NaCl solution using electrochemical impedance spectroscopy (EIS). The synergism effect of nanoparticles along with PPy resulted in an enhancement of mechanical and corrosion-resistant properties.

**Keywords:** coating; epoxy; conducting polymer; nanoparticle; corrosion; nano-indentation

## 1. Introduction

The three-layer coating system with poor surface preparation and application may lead to blistering, pinholes, peeling, lifting due to the poor adhesion to the substrate or due to the inter-coat adhesion. The use of corrosion inhibiting pigments causes environmental hazards; also, a very high quantity of anticorrosive pigment is required to achieve the anticorrosive properties for metal protection. On the other hand, the presence of highly conductive polymers or nanofillers such as carbon nanotubes in coatings can significantly increase their corrosion protection in a more environmentally friendly way [1,2]. Nevertheless, problems with the proper distribution of nanofillers in coating compositions partially limit their usability and force researchers to seek such solutions in which nanofillers could be

one of a few raw materials that increase coating properties [3]. Therefore, more processable conducting polymers have been introduced as a choice to get rid of the detrimental hazards of corrosion-inhibiting pigments. Conjugated conducting polymer (CP) have attracted huge interest both in academic and research topics recently for their various applications such as corrosion protection, light-emitting diodes, sensors and actuators, electromagnetic interference shielding and electrostatic charge dissipation, catalysts and energy conversion systems [4–10]. Mengoli et al. [11] and DeBerry [12] demonstrated firstly that CP can be used in corrosion control, and that an intensive effort has been carried out to expand such coating systems. Partially, this has been provoked by the need to substitute chromium (VI)-based coatings for corrosion control of iron and aluminum alloys. A Cr (VI) compound like chromate is the most efficient common corrosion inhibitor. Coatings based on conducting polymers like polyaniline, polypyrrole, etc., shows potential alternates for Cr (VI)-based coatings, attributable to their redox properties and conductivity. Several research works have been accomplished with CP addition to control the corrosion of non-ferrous metals [9] and ferrous metals [10].

CP seems an innovative materials class which offers a sole set of new properties. The main advantages of CP are low density, thermal and chemical stability and the ease of synthesis. These polymer-based coatings are able to congregate high demands and are the best conventional anti-corrosion coating systems. Common CP are polyacetylene, polypyrrole, polythiophene, poly(p-phenylene) and polyaniline. Among them Polyaniline (PANI) is the most accepted as it has very good corrosion protective properties for coatings [11–13]. Extensive work has already been performed and reported with polyaniline-based epoxy coatings along with suitable nano-particles such as ZnO and its synergistic effect with Ag nanoparticles. Ag and ZnO nanoparticles were incorporated to obtain superior mechanical and corrosion-resistance properties. The findings resulted in an enhancement in mechanical and corrosion resistance for the final coating [14].

This work is motivated by the properties of CP and their higher solubility in general conducting polymers. Therefore, we believe that the solubility or dispensability of CP might reveal a new area for its application as an anticorrosion pigment. Here, our intention is to develop a coating containing a conducting polymer based nanocomposites (e.g., CP-inorganic parts like Ag, ZnO etc.) as the anticorrosive pigment to replace the conventional coatings used in this field. Ates et al. [15] produced PANI based nanocomposites with the incorporation of inorganic nanoparticles of TiO<sub>2</sub>, Ag and Zn by vapor deposition method. The nanocomposite films of the PANI, PANI/TiO<sub>2</sub>, PANI/Ag and PANI/Zn were immersed in 3.5% NaCl solution for a certain time interval and investigated for corrosion-resistant properties [16]. The results were evaluated with Tafel extrapolation and electrochemical impedance spectroscopy (EIS) techniques. The results exhibited that PANI/Ag nanocomposite films yielded higher corrosion resistance properties (protection efficiency, PE = 97.54%) as compared to PANI (PE = 91.41%), PANI/TiO<sub>2</sub> (PE = 91.91%), and PANI/Zn (PE = 92.52%) nanocomposite films [15]. The PANI composition with nanomaterials (TiO<sub>2</sub>, Ag and Zn) resulted in an enhancement of electrical conductivity of the PANI/Zn film and the protection efficiency or corrosion resistance of the polyaniline polymer. These findings were further confirmed by decreasing the oxygen and water permeability and increasing coating adhesion in the presence of TiO<sub>2</sub>, Ag and Zn nanomaterials in the PANI. The incorporation of TiO<sub>2</sub>, Ag, and Zn into the coating increased both the charge transfer and pore resistance, measured by the EIS technique. The PANI/Ag nanocomposite film (PE = 97.54%) showed higher corrosion resistance which was compared and reported. The results showed better corrosion resistance efficiency of Ag-incorporated nano-coatings as compared to others. This research motivated our work [17] to incorporate the conductive polymer (PPy) with Ag and ZnO and to develop the formulations of their synergism in order to achieve balanced and improved corrosion-resistance properties for offshore or splash-zone applications.

Therefore, we would like to evaluate the performance of conducting polymers along with nano-pigments in epoxy matrix against saline corrosion of steel that are commonly used to protect tanks and pipelines. Observations by electrochemical impedance spectroscopy have been used to understand their effectiveness. Thus, we observed, that the CP-based nanocomposites coating can be

used for corrosion protection of steel with safety, with environmental benefits and with intention of replacing hazardous corrosion inhibiting pigments.

## 2. Materials and Methods

The polypyrrole (PPy) used for the formulation was doped, composite with carbon black (530573) purchased from Sigma-Aldrich (Gillingham, Dorset, UK). PPy based formulations were prepared and coated on a metal substrate. Each of these formulations includes a bisphenol-A based epoxy resin and compatible solvents like xylene, methyl isobutyl ketone (MIBK), for homogeneous mixing, leveling agent and de-foamer. Epoxy resin DGEBA, polyamidoamine adduct hardener, MIBK, xylene, and acetone were procured from local suppliers. A small amount of acetone was used to disperse nanoparticles, in acetone 1% by weight of silane was added and stirred for 5 min at low rpm using mechanical mixer. After 5 min, Ag and ZnO nanoparticles (purchased from Sigma-Aldrich) were added to the solvent (after dispersion of first nanoparticles) and mixed for 15 min to facilitate complete dispersion. These dispersed nanoparticles were then added to epoxy/PPy mixture and stirred at 4000 rpm to mix the nanoparticles in epoxy matrix. After mixing the formulation was subjected to sonication for at least 20 min. After completing sonication, the formulation was left to stabilize. After stabilization, hardener was mixed to epoxy/PPy /nanoparticle formulation and mixed using mechanical stirrer at 500 rpm for 5–6 min. Epoxy and hardener were mixed in a 5:1 (epoxy:hardener) ratio This modified slurry was coated onto prepared mild steel substrates for characterization, taking into account that the mixture should be stabilized before being applied as a coating. The application of the coatings was carried out using an automatic film applicator, Sheen Instruments, Cambridge, UK. The formulations of ingredients and nanoparticles are listed in Table 1.

**Table 1.** Epoxy/2pack coating incorporated with polypyrrole (PPy), Ag and ZnO nanoparticles.

Sample	Epoxy Resin	PPy Wt%	Xylene	MIBK	Dispersing Agent	Silane Wt.%	Nano Ag	Nano ZnO	Hardener D-3282 Wt.%
Epoxy-PPy	83.34	0.95	10	10	1	1	0	0	16.66
F1	83.34	0.95	10	10	1	1	0.2	0.2	16.66
F2	83.34	0.95	10	10	1	1	0.4	0.4	16.66

X-ray diffraction (XRD) measurements using Cu K $\alpha$  analysis were taken for coating samples to confirm the presence of nanoparticles in the epoxy coatings, using a broker D8 discover diffractometer (Bruker, Olaya, Saudi Arabia) operated at 40 kV/40 mA. The scans were performed at room temperature within the range 2 $\theta$  of 10°–80° and at a speed of 2°/min. The hardness and modulus of elasticity for the formulae were evaluated employing the nano-indentation technique. Nano-indenter from micro materials was used to measure elastic modulus and hardness of prepared coatings for nanoparticles incorporated epoxy/PPy coatings. A Berkovich-type indenter was used to test the coatings. A load-controlled program was used to obtain indentations, coating samples were subjected to maximum load of 250 mN at 1 mN/s loading rate, the applied load was held at its maximum for 60 s. The indenter was withdrawn from the coating at the same rate (1 mN/s) until the load is completely removed. At least 15 indentations were made on the coatings sample to obtain consistency in the results. Final results are averaged of all the indentations performed. The corrosion behavior of the epoxy coatings was reported by the use of the non-traditional EIS measurements. These measurements were performed in a conventional three-electrode cell that has an Ag/AgCl (in a saturated KCl solution) as a reference electrode, stainless steel sheet as a counter electrode, and steel-epoxy coated coupons as working electrodes. The EIS data were collected after varied exposure periods of time (1 h to 30 days) in 3.5% NaCl solutions using an Autolab Ecochemie PGSTAT 30 (Metrohm, Amsterdam, The Netherlands), and a frequency scan within the range of 100,000 to 0.1 Hz. The EIS experiments were carried out by applying a  $\pm 5$  mV amplitude sinusoidal wave perturbation at the corrosion potential.

### 3. Results and Discussion

#### 3.1. Mechanical Properties

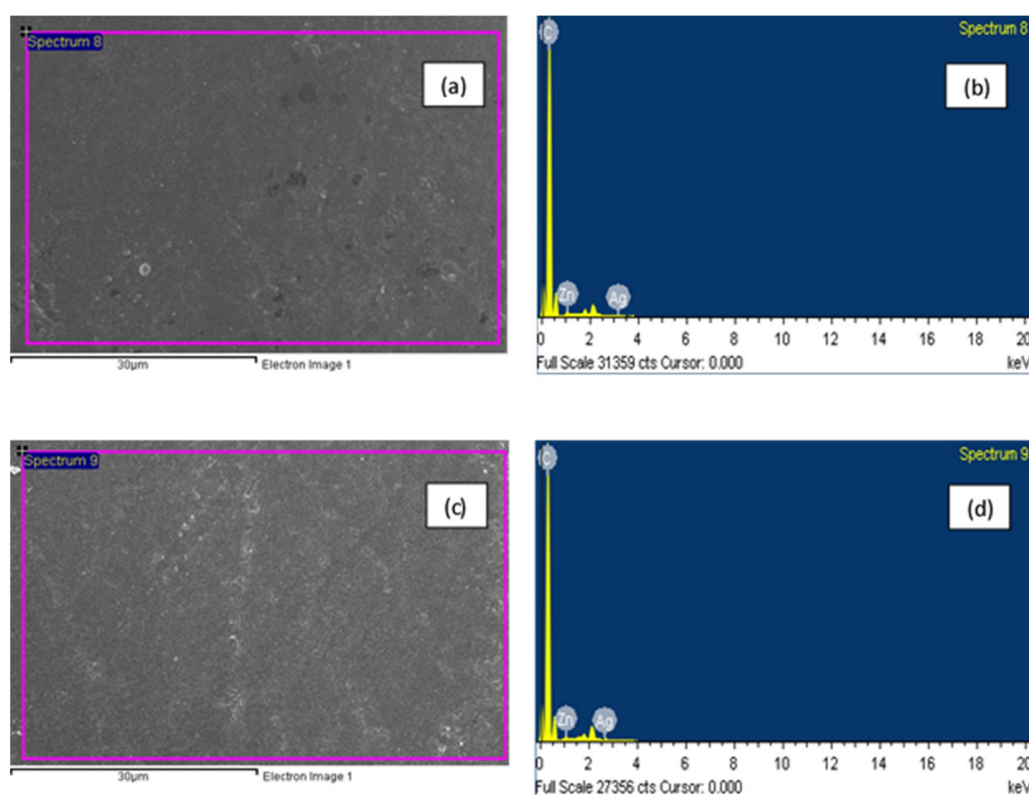
After 7 days of curing the coated panels were subjected to mechanical characterization. As can be seen in Table 2, the obtained results suggest an increase in all mechanical properties as compared to our base formulation [17]. The increase in these properties can be attributed to the addition of ZnO nanoparticles as literature suggests ZnO enhances the mechanical properties [18,19].

**Table 2.** Obtained values of dry film thickness, pendulum hardness, scratch resistance, and impact strength for the different ZnO and Ag-incorporated epoxy PPy coatings.

Samples	PPy	Nanoparticles		Dry Film Thickness (DFT) ( $\mu\text{m}$ )	Pendulum Hardness (Oscillations)	Scratch Resistance (Kg)	Impact Strength (Kg/cm)
		Ag	ZnO				
Epoxy/PPy	0.95%	0	0	60–80	135	5	3.37
F1	0.95%	0.2%	0.2%	70–90	145	8	11.43
F2	0.95%	0.4%	0.4%	70–90	153	7	12.86

#### 3.2. Surface Morphology and X-ray Diffraction (XRD) Spectroscopy

The EDX spectra for neat epoxy coated sample shown in Figure 1 as a whole is identified as carbon and oxygen and there is no other element identified in the pure epoxy coating. The elemental analysis by EDX confirms the presence of nanoparticles (Ag and Zn) in the nanocomposite coated samples (F1 and F2) as shown in Figure 1. The elements identified by EDX studies with an approximate weight percent of the elements are shown in Table 3.

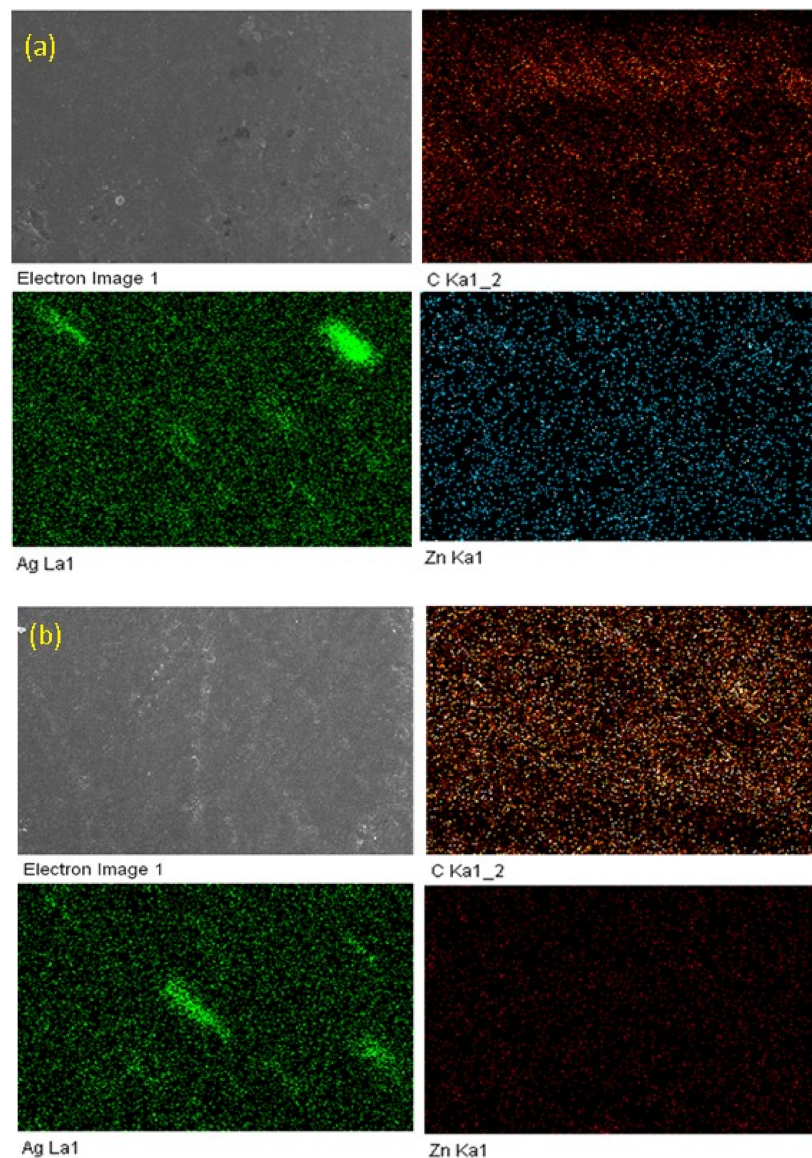


**Figure 1.** (a,c) Scanning electron microscope (SEM) images where energy dispersive X-ray spectroscopy (EDX) was performed, (b,d) EDX spectra obtained for F1 and F2 samples.

**Table 3.** Elemental analysis and wt.% of elements by EDX.

Sample	Nano Particles	Elements Present	Weight %
F1	Ag, Zn	C, Zn, Ag	99.10, 0.59, 0.31,
F2	Ag, Zn	C, Zn, Ag	98.82, 0.85, 0.33,

The presence of the nanoparticles Ag & ZnO found at the surface, and the distribution of these particles in epoxy coatings confirms the incorporation in final formulations. Figure 2a,b shows the SEM image of area at which EDX mapping spectra was obtained for F1 and F2 formulations. The percentages were found to be C (99.10%), Ag (0.31%), Zn (0.59%) for F1 and C (98.82%), Ag (0.33%), Zn (0.85%) for the F2 formulation respectively. The presence of carbon (C) is in abundance in both formulations due to epoxy matrix (DGEBA), curing agent (D-3282), and PPy as their backbone constituent. The percentage of Ag and Zn are slightly higher than that originally present in F1 and F2 coatings, because of particle aggregation at the surface of epoxy coatings. The mapping images as shown in Figure 2 and presence of nanoparticles depicted the overall distribution uniformly, which resulted in better performance as compared to epoxy/PPy coating.

**Figure 2.** (a,b) EDX mapping for F1 and F2 samples.

The XRD patterns of ZnO and Ag nanoparticles, and the prepared formulations of epoxy/PPy, F1 and F2, are shown respectively in Figure 3. It is shown in Figure 3, which was performed for the ZnO powder nanoparticles, that the standard peaks are observed at  $2\theta$  of  $31.70^\circ$ ,  $34.25^\circ$ ,  $36.20^\circ$ ,  $47.45^\circ$ ,  $56.57^\circ$ ,  $62.70^\circ$ ,  $66.30^\circ$  and  $67.86^\circ$  respectively. Also, the standard peaks of the powder Ag nanoparticles are detected at  $2\theta$  of  $38.10^\circ$ ,  $44.0^\circ$ ,  $64.40^\circ$ ,  $77.30^\circ$ , respectively. The XRD spectra of epoxy/PPy does not show any characteristic peak instead a broadline spectra was obtained. The incorporation of both ZnO and Ag nanoparticles can be seen in the F1 and F2 formulations given in the figure, clearly stating the presence of these nanoparticles in the matrix at the  $2\theta$  values. The intensity difference in both F1 and F2 coatings shows the difference in amounts of nanoparticles as F2 gives higher intensity peaks. No peak shift was observed during the analysis, which suggests that the incorporation of these nanoparticles did not alter the chemical composition of the matrix. Also the miller planes obtained from XRD are in accordance with the standard XRD planes for Ag and ZnO.

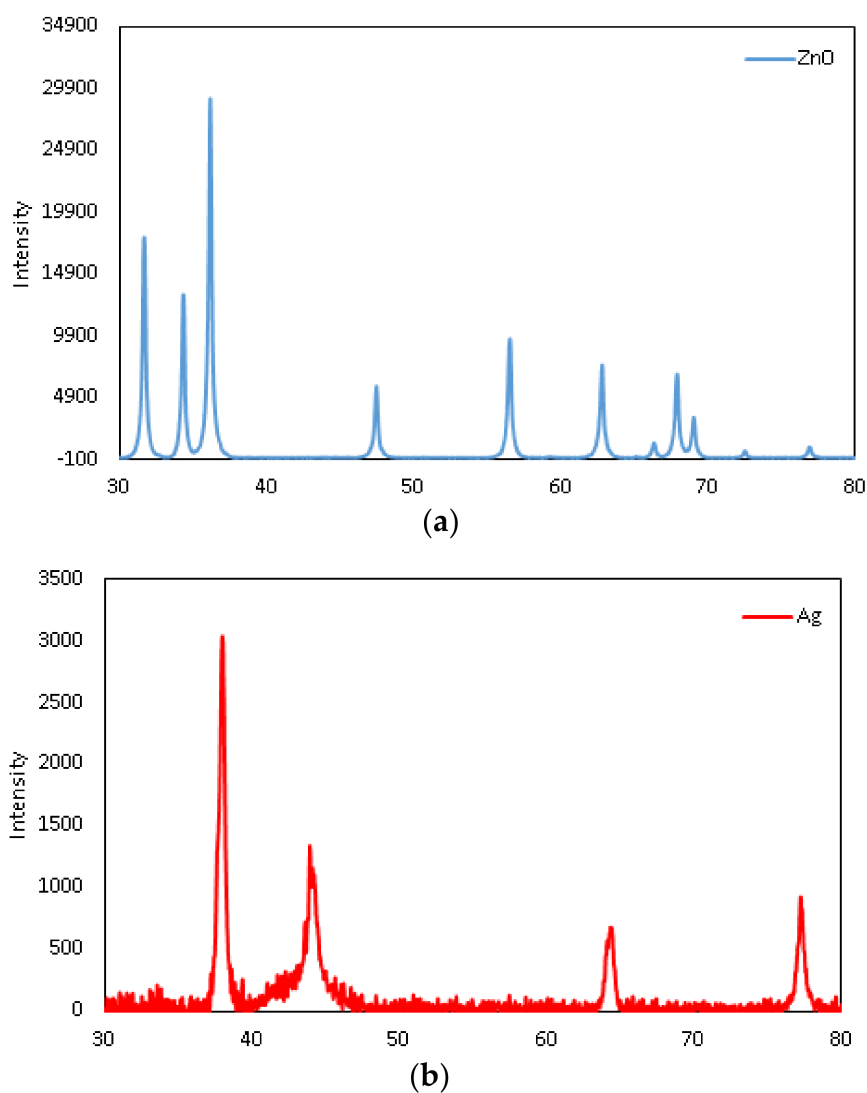
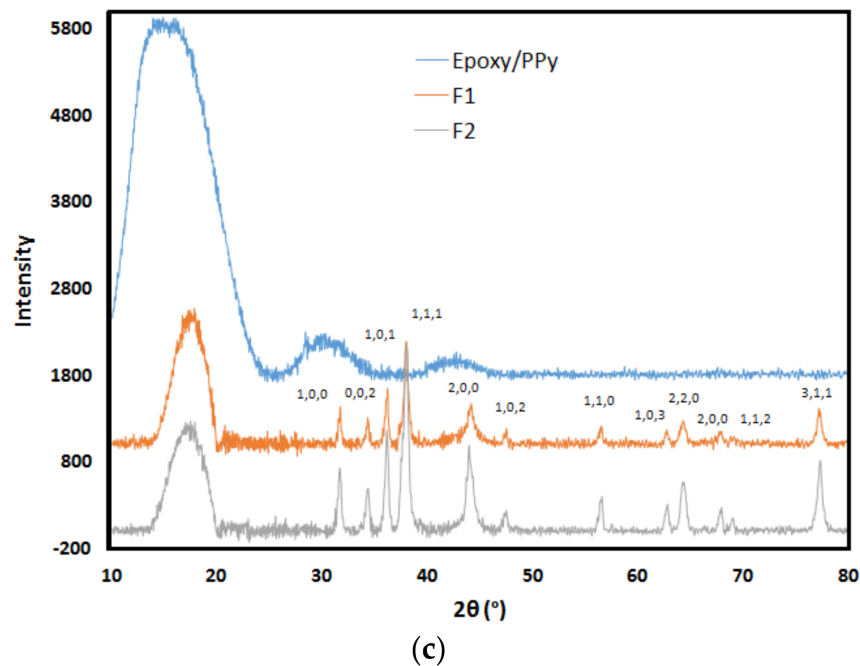


Figure 3. Cont.



**Figure 3.** X-ray diffraction (XRD) patterns of (a) ZnO nanoparticles, (b) Ag nanoparticles, and (c) the prepared formulations of epoxy/PPy, F1, and F2.

### 3.3. Nanoindentation Analysis

Figure 4 below shows the load vs. displacement curve of nanoindentation test performed, as can be seen the load-bearing capacity is higher in F2 formulation incorporated with nanoparticles, but lower than epoxy/PPy formulation. The maximum depth achieved at 250 mN load for both samples were 8154 nm for F2, while 8417 nm for F1 was recorded, while 7493 nm for epoxy/PPy coating. This shift towards lower depth values is because of the presence of nanoparticles in formulation. The shifting of graph to lower depth value suggests an increase in load-bearing capacity of the coating [20,21].

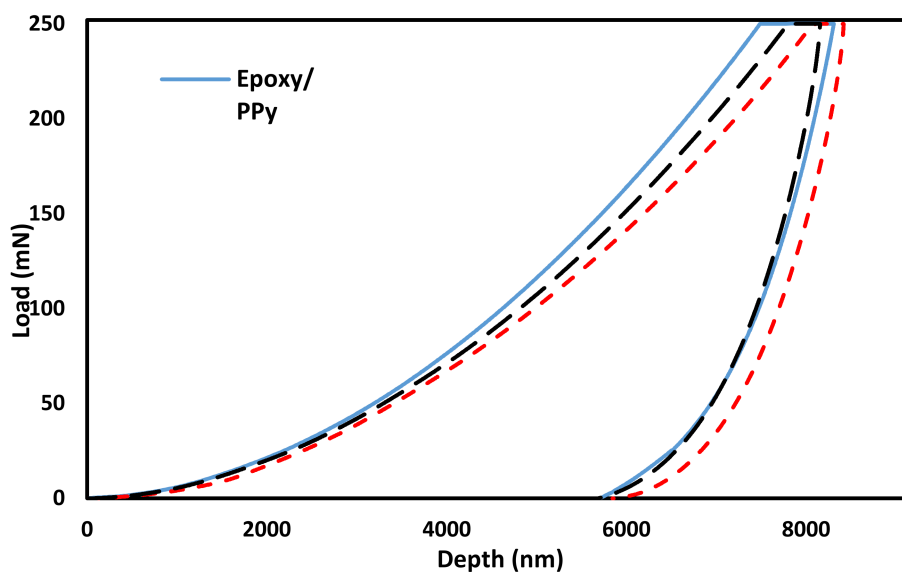


**Figure 4.** Nanoindentation load vs. depth graph for the fabricated epoxy/PPy, F1, and F2 coatings.

Modulus and hardness properties upon incorporation of the nanoparticles were extracted from load vs depth curves using software provided by micro-material UK. The software works on the principle of Oliver and Pharr [22] method. Hardness and elastic modulus were calculated according to Equations (1) and (2):

$$H = F_{\max}/A_c \quad (1)$$

where,  $H$  = Hardness,  $F_{\max}$  = maximum load applied, and  $A_c$  = Projected contact area

$$1/E_r = (1 - \nu^2)/E + (1 - \nu_i^2)/E_i \quad (2)$$

$E_r$  is reduced modulus.  $E$  and  $E_i$  are elastic modulus of sample and indenter  $\nu$  and  $\nu_i$  are Poisson's ratio of sample and diamond indenter, respectively.

Figure 5 shows graphical representation of hardness and elastic modulus, while Table 4 shows the values obtained after indentation test. As can be seen in the figure, the formulation containing a higher amount of nanoparticles possesses higher indentation hardness ( $F2 = 0.18$  GPa) but it is still lower than the epoxy coatings without nanoparticles, while a reasonable improvement in modulus was witnessed with higher nanoparticles percentage. This increase in hardness and the improvement in modulus values are due to nanoparticles addition, as nanoparticles takes up free volume in matrix and restricts chain mobility [19,23,24]. The results obtained are in accordance with the mechanical properties described above, where an increase in nanoparticles amounts to an increase in pendulum hardness and scratch resistance. The results suggest that increasing amount of nanoparticles in epoxy is responsible in enhancing surface properties of coatings and making it difficult to be affected by external stimuli. The higher hardness and lower modulus values for epoxy/PPy may be attributed to indentation size and the area at which the test is performed. There is a possibility of indenter landing at an area where particles were agglomerated because of its smaller size, resulting in higher hardness and lower modulus properties. The results obtained for indentation are not in accordance with the mechanical properties for conventional testing as results indicated in Table 2.

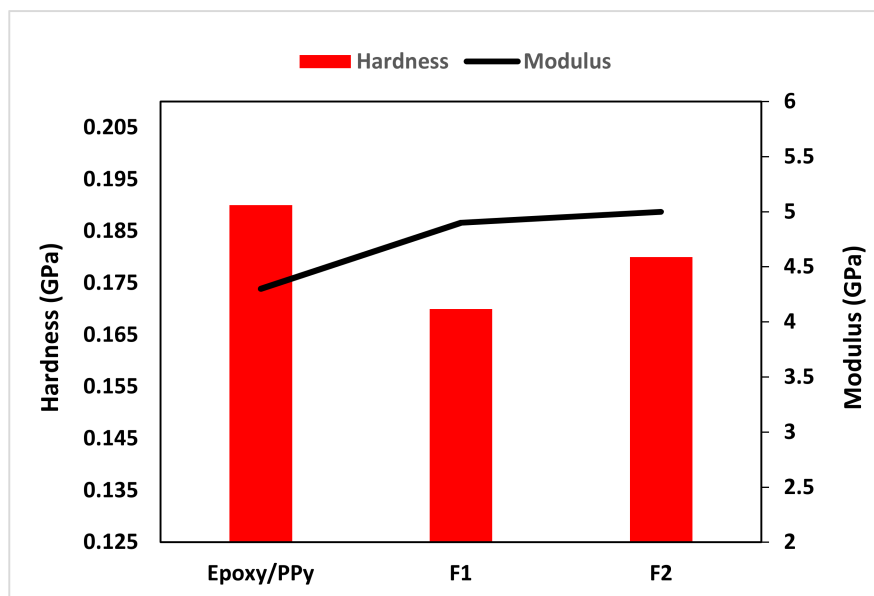


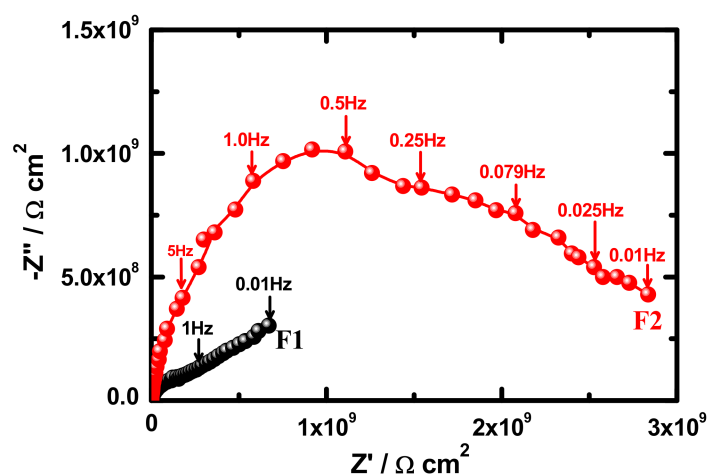
Figure 5. Nanoindentation analysis for the fabricated epoxy/PPy, F1, and F2 coatings.

**Table 4.** Micro-hardness and reduced modulus recorded for the fabricated epoxy coatings (F1 and F2) containing Ag and ZnO nanoparticles.

Sample	Nanoparticle		Hardness (GPa)	Elastic Modulus (GPa)
	Ag	ZnO		
Epoxy/PPy	0.0	0.0	0.19	4.3
F1	0.2%	0.2%	0.17	5.0
F2	0.4%	0.4%	0.18	4.9

### 3.4. Electrochemical Impedance Spectroscopy (EIS)

EIS measurements have been successfully employed to report the kinetic parameters for the electron transfer at the surface/electrolyte interface [14,25–30]. The Nyquist plots obtained for F1 and F2 epoxy coating incorporated Ag and ZnO nanoparticles after 1 h immersion in 3.5% NaCl solution are shown in Figure 6. The epoxy coating that contains 0.2% Ag and 0.2% ZnO (F1) depicted only one semicircle with a small diameter. On the other hand, increasing Ag and ZnO in the coating to 0.4% each, F2 sample, increased the diameter of the obtained semicircle. This indicates that the increase of percent of both Ag and ZnO increases the corrosion resistance for the epoxy coating. The increase of corrosion resistance is due to a synergistic effect of Ag and ZnO nanoparticles within the coating structure, which increases with the increase of Ag and ZnO contents [14].

**Figure 6.** Nyquist plots obtained for coatings F1 and F2 after 1 h immersion in the 3.5% NaCl solutions.

In order to study the effect of prolonging the exposure periods of time on the corrosion behavior of the fabricated coatings, impedance measurements were carried out after 7, 15, 21 and 30 days and the spectra are shown in Figures 7–10, respectively. It is seen from Figure 7 that increasing the immersion time to 7 days decreases the corrosion resistance for F1 and F2 epoxy coatings. The decrease in the corrosion resistance is most probably due to the degradation of the surface of the coating as a result of being exposed for long period of time in the chloride test solution, because of water diffusion into the coating [31]. This was confirmed by the spectra shown in Figures 8–10 that were obtained for the epoxy coatings after being immersed for 15, 21 and 30 days, respectively. It is clear from all EIS spectra that the increase of the content of Ag and ZnO nanoparticles decreases the corrosion of the epoxy coatings and thus increases the corrosion resistance as a result of a synergetic effect occurs between the epoxy coating and Ag with ZnO nanoparticles together [14]. Although, the increase of time of exposure before measurement leads to degrading the surface of the coatings, the corrosion resistance for the F2 coating is higher than that obtained for the F1 sample.

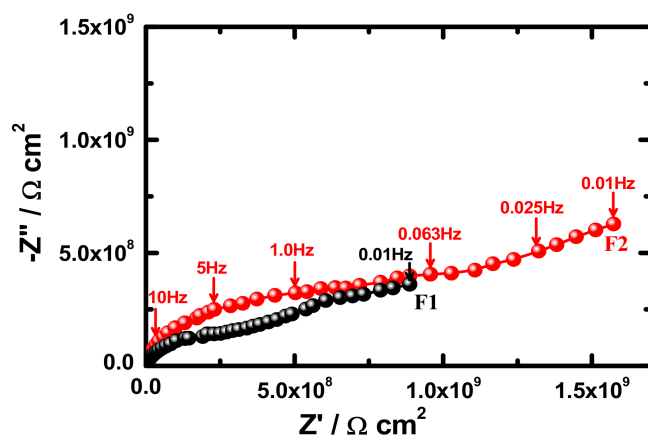


Figure 7. Nyquist plots for coatings F1 and F2 after 7 days' immersion in the 3.5% NaCl solutions.

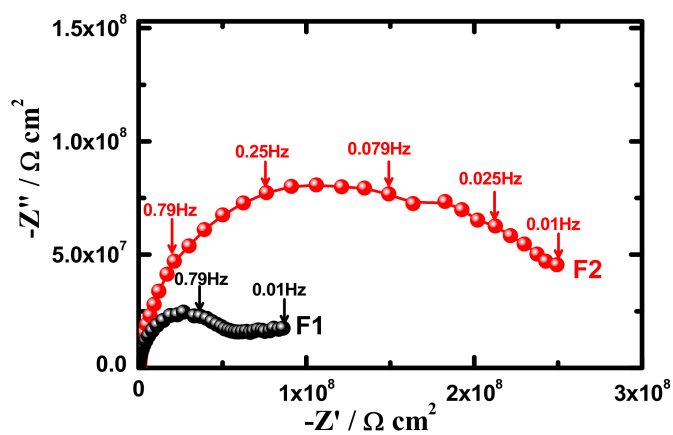


Figure 8. Nyquist plots for coatings F1 and F2 after 15 days' immersion in the 3.5% NaCl solutions.

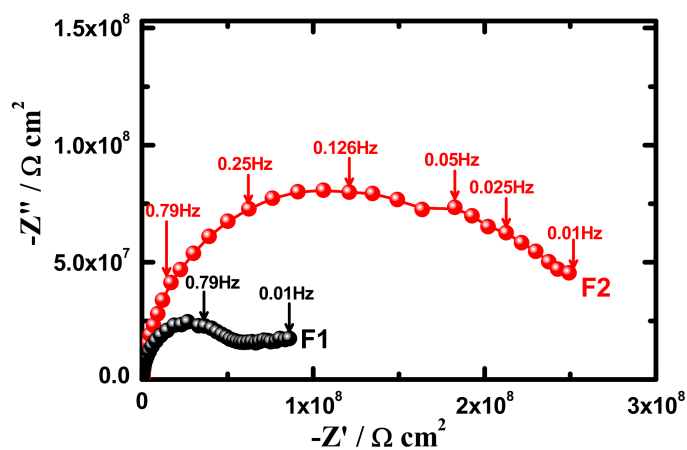


Figure 9. Nyquist plots for coatings F1 and F2 after 21 days' immersion in the 3.5% NaCl solutions.

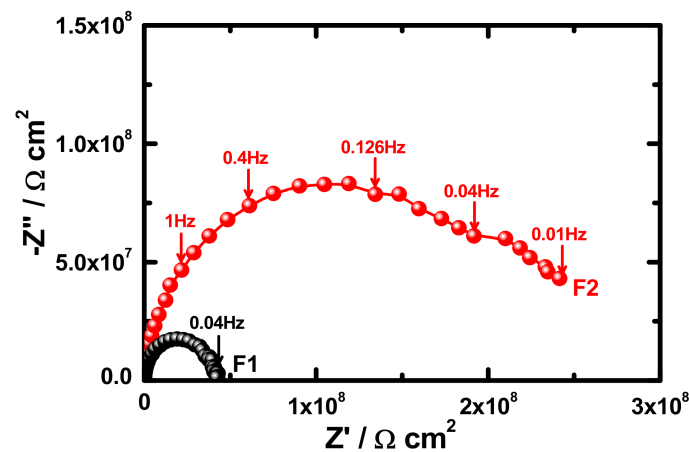


Figure 10. Nyquist plots for coatings F1 and F2 after 30 days immersion in the 3.5% NaCl solutions.

The EIS results were best fitted to the equivalent circuit model as presented in Figure 11. The symbols represented on the equivalent circuit are defined as follows; a solution resistance ( $R_s$ ), constant phase elements ( $Q_1$ ), polarization resistance ( $R_{P1}$ ), another constant phase element ( $Q_2$ ), a second polarization resistance ( $R_{P2}$ ), and Warburg impedance ( $W$ ). The values of these symbols are listed in Table 5. It is clear from the Nyquist plots and Table 5 that the increase of the concentration of Ag to 0.4% and ZnO to 0.4% increases the values of all resistances,  $R_s$ ,  $R_{P1}$  and  $R_{P2}$ . It is reported [25,28] that  $R_{P1}$  is the charge transfer resistance and represents the polarization resistance between the epoxy coatings and the interface of the solution, while  $R_{P2}$  is the resistance between the layer of corrosion product and the solution. The overall polarization resistance is obtained from the parallel combination of  $R_{P1}$  and  $R_{P2}$ . This effect also decreases the values of  $Y_{Q1}$ , where  $Q_1$  represents double layer capacitors as their  $n$  values are close to unity. Also, the values of  $Y_{Q2}$  decreased and  $Q_2$  can be considered as the Warburg impedance as their  $n$  values are around 0.5. The presence of  $W$  indicated also that the surfaces of the fabricated epoxy coatings have excellent corrosion resistance and the corrosion of the coatings does not take place via the dissolution of the surface of the coatings.

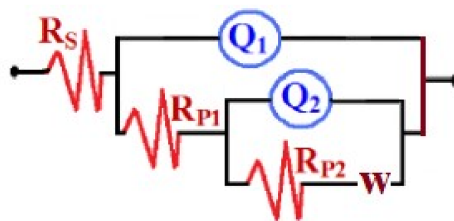


Figure 11. The equivalent circuit model used to fit electrochemical impedance spectroscopy (EIS) data.

Table 5. EIS parameters obtained by fitting the Nyquist plots for the different epoxy coatings immersed in 3.5% NaCl solutions for varied exposure periods.

Samples	$R_s/\Omega\text{cm}^2$	$Q_1$		$R_{P1}/k\Omega\text{cm}^2$	$Q_2$		$R_{P2}/k\Omega\text{cm}^2$	$W/\Omega\text{S}^{-1/2}$
		$Y_{Q1}/\text{Fcm}^{-2}$	$n^1$		$Y_{Q2}/\text{Fcm}^{-2}$	$n^2$		
F1 (1 h)	95	$1.29 \times 10^{-10}$	0.94	8999	$2.76 \times 10^{-9}$	0.45	1596	$1.93 \times 10^{-9}$
F2 (1 h)	104	$7.86 \times 10^{-11}$	0.98	9794	$1.08 \times 10^{-9}$	0.43	2432	$6.29 \times 10^{-9}$
F1 (7 days)	96	$1.19 \times 10^{-10}$	0.95	6603	$2.09 \times 10^{-9}$	0.42	1568	$3.29 \times 10^{-9}$
F2 (7 days)	103	$1.48 \times 10^{-10}$	0.91	7732	$6.15 \times 10^{-9}$	0.43	2351	$2.68 \times 10^{-9}$
F1 (15 days)	87	$1.57 \times 10^{-9}$	0.97	5468	$2.56 \times 10^{-9}$	0.48	1497	$7.11 \times 10^{-9}$
F2 (15 days)	101	$5.13 \times 10^{-9}$	0.94	6336	$3.10 \times 10^{-9}$	0.44	2145	$5.31 \times 10^{-9}$
F1 (21 days)	85	$1.59 \times 10^{-9}$	0.97	4595	$1.03 \times 10^{-8}$	0.39	1335	$5.17 \times 10^{-9}$
F2 (21 days)	105	$2.57 \times 10^{-9}$	0.97	6161	$6.04 \times 10^{-9}$	0.44	1931	$3.06 \times 10^{-9}$
F1 (30 days)	85	$2.02 \times 10^{-9}$	0.98	3254	$3.3 \times 10^{-8}$	0.41	1096	$4.68 \times 10^{-9}$
F2 (30 days)	103	$3.15 \times 10^{-9}$	0.95	5465	$2.29 \times 10^{-8}$	0.45	1512	$1.37 \times 10^{-9}$

The EIS data collectively confirmed that the increase of Ag and ZnO contents from 0.2% to 0.4% greatly increases the passivation of the coatings. This passivation process is mainly due to the presence of both Ag and ZnO together, which could lead to a synergetic effect between those nano particles and the epoxy coating. It is worth mentioning also that the presence of Ag nanoparticles alone did not produce the same effect on the corrosion performance of polyurethane (PU) coating film as has been previously claimed by Akbarian et al. [32]. The authors [32] have reported that the addition of Ag nanoparticles within two different epoxy coatings; namely the high solid PU and waterborne (WP) coatings, resulted in no significant effect on the corrosion protection behavior of PU and an acceleration effect represented by a severe deterioration of the WP coating film when PU and WP were incorporated with silver nanoparticles and were individually applied onto steel surfaces then exposed to 3.5% NaCl solutions. The difference between our findings and that reported earlier [31] on the effect of the silver nanoparticles-incorporated epoxy coatings is the presence of ZnO nanoparticles that could lead to the occurrence of a synergistic effect that enhances both the ability of Ag and ZnO together to better protect the coated surfaces.

#### 4. Conclusions

Accelerated corrosion assays using an aggressive 3.5% saline solution revealed that the panels coated (F1 and F2) with PPy-based epoxy coatings (a synergism of Ag and ZnO nanoparticles) are significantly more resistant against corrosion than those protected with the epoxy conventional coatings. Therefore, results also revealed that some conducting polymer compositions F1 and F2 can inhibit the steel corrosion and small concentrations of these materials may be used to replace conventional inorganic corrosion inhibitors currently used in an epoxy system. On the other hand, comparison with the accelerated corrosion results previously reported for different coatings which were obtained using identical experimental conditions also revealed that the incorporation of nanoparticles and synergism of (Ag, ZnO) and the addition of the CP (PPy) produces a benefit in terms of corrosion protection, especially for the sample F2.

**Author Contributions:** Conceptualization, M.A.A.; Methodology, M.A.A. and U.A.S.; Formal Analysis, M.A.A., U.A.S., E.-S.M.S. and H.S.; Writing—Original Draft Preparation, M.A.A., U.A.S., E.-S.M.S. and H.S.; Writing—Review and Editing, U.A.S., E.-S.M.S. and M.A.; Supervision, N.H.A. and S.M.A.-Z.; Project Administration, S.M.A.-Z.

**Funding:** This work is funded by the Deanship of Scientific Research at King Saud University through the Research Group Project No. RGP-160.

**Acknowledgments:** The authors would like to extend their sincere appreciation to the Deanship of Scientific Research at King Saud University for its funding of this research through the Research Group Project No. RGP-160.

**Conflicts of Interest:** The authors declare no conflict of interest.

#### References

1. Armelin, E.; Pla, R.; Liesa, F.; Ramis, X.; Iribarren, J.I.; Alemán, C. Corrosion protection with polyaniline and polypyrrole as anticorrosive additives for epoxy paint. *Corros. Sci.* **2008**, *50*, 721–728. [[CrossRef](#)]
2. Kugler, S.; Kowalczyk, K.; Spychaj, T. Transparent epoxy coatings with improved electrical, barrier and thermal features made of mechanically dispersed carbon nanotubes. *Prog. Org. Coat.* **2017**, *111*, 196–201. [[CrossRef](#)]
3. Chang, C.-H.; Huang, T.-C.; Peng, C.-W.; Yeh, T.-C.; Lu, H.-I.; Hung, W.-I.; Weng, C.-J.; Yang, T.-I.; Yeh, J.-M. Novel anticorrosion coatings prepared from polyaniline/graphene composites. *Carbon* **2012**, *50*, 5044–5051. [[CrossRef](#)]
4. Greenham, N.C.; Moratti, S.C.; Bradley, D.D.C.; Friend, R.H.; Holmes, A.B. Efficient light-emitting diodes based on polymers with high electron affinities. *Nature* **1993**, *365*, 628–630. [[CrossRef](#)]
5. Koul, S.; Chandra, R.; Dhawan, S.K. Conducting polyaniline composite for ESD and EMI at 101 GHz. *Polymer* **2000**, *41*, 9305–9310. [[CrossRef](#)]
6. Glatthaar, M.; Niggemann, M.; Zimmermann, B.; Lewer, P.; Riede, M.; Hinsch, A.; Luther, J. Organic Solar Cells Using Inverted Layer Sequence. *Thin Solid Film.* **2005**, *491*, 298–300. [[CrossRef](#)]

7. Mengoli, G.; Munari, M.T.; Bianco, P.; Musiani, M.M. Anodic synthesis of polyaniline coatings onto Fe sheets. *J. Appl. Polym. Sci.* **1981**, *26*, 4247–4257. [[CrossRef](#)]
8. DeBerry, D.W. Modification of the Electrochemical and Corrosion Behavior of Stainless Steels with an Electroactive Coating. *J. Electrochem. Soc.* **1985**, *132*, 1022–1026. [[CrossRef](#)]
9. Tallman, D.E.; Spinks, G.; Dominis, A.; Wallace, G.G. Electroactive Conducting Polymers for Corrosion Control Part 1. General Introduction and a Review of Non-ferrous Metals. *J. Solid State Electrochem.* **2002**, *6*, 73–84. [[CrossRef](#)]
10. Spinks, G.M.; Dominis, A.J.; Wallace, G.G.; Tallman, D.E. Electroactive conducting polymers for corrosion control. *J. Solid State Electrochem.* **2002**, *6*, 85–100. [[CrossRef](#)]
11. Lu, W.K.; Elsenbaumer, R.L.; Wessling, B. Corrosion protection of mild steel by coatings containing polyaniline. *Synth. Met.* **1995**, *71*, 2163–2166. [[CrossRef](#)]
12. Dhawan, S.K.; Trivedi, D.C. Synthesis and characterization of poly(o-ethoxyaniline): A processable conducting polymer. *J. Appl. Polym. Sci.* **1995**, *58*, 815–826. [[CrossRef](#)]
13. Daouadji, M.M.; Chelali, N. Influence of molecular weight of poly(ortho-ethoxyaniline) on the corrosion inhibition efficiency of mild steel in acidic media. *J. Appl. Polym. Sci.* **2004**, *91*, 1275–1284. [[CrossRef](#)]
14. Alam, M.A.; Samad, U.A.; Sherif, E.-S.M.; Seikh, A.; Al-Zahrani, S.M.; Alharthi, N.H.; Alam, M. Synergistic effect of Ag and ZnO nanoparticles on polyaniline incorporated epoxy/2pack coatings for splash zone applications. *J. Coat. Technol. Res.* **2019**, in press. [[CrossRef](#)]
15. Ates, M.; Topkayaa, E. Nanocomposite film formations of polyaniline via TiO<sub>2</sub>, Ag and Zn, and their corrosion protection properties. *Prog. Org. Coat.* **2015**, *82*, 33–40. [[CrossRef](#)]
16. Gomez, H.; Ram, M.K.; Alvi, F.; Stefanakos, E.; Kumar, A. Novel synthesis, characterization, and corrosion inhibition properties of nano-diamond-polyaniline films. *J. Phys. Chem. C.* **2010**, *114*, 18797–18804. [[CrossRef](#)]
17. Alam, M.A.; Samad, U.A.; Sherif, E.-S.M.; Alothman, O.; Seikh, A.H.; Al-Zahrani, S.M. Effects of minor additions of polypyrrole on the thermal, mechanical and electrochemical properties of epoxy-2pack coatings. *Int. J. Electrochem. Sci.* **2017**, *12*, 74–89. [[CrossRef](#)]
18. Karasinski, E.N.; Da Luz, M.G.; Lepienski, C.M.; Coelho, L.A.F. Nanostructured coating based on epoxy/metal oxides: Kinetic curing and mechanical properties. *Thermochim. Acta.* **2013**, *569*, 167–176. [[CrossRef](#)]
19. Samad, U.A.; Alam, M.A.; Chafidz, A.; Al-Zahrani, S.M.; Alharthi, N.H. Enhancing mechanical properties of epoxy/polyaniline coating with addition of ZnO nanoparticles: Nanoindentation characterization. *Prog. Org. Coat.* **2018**, *119*, 109–115. [[CrossRef](#)]
20. Samad, U.A.; Alam, M.A.; Sherif, E.-S.M.; Alothman, O.; Seikh, A.H.; Al-Zahrani, S.M. Manufacturing and characterization of corrosion resistant epoxy/2pack coatings incorporated with polyaniline conductive polymer. *Int. J. Electrochem. Sci.* **2015**, *10*, 5599–5613.
21. Shen, L.; Wang, L.; Liu, T.; He, C. Nanoindentation and morphological studies of epoxy nanocomposites. *Macromol. Mater. Eng.* **2006**, *291*, 1358–1366. [[CrossRef](#)]
22. Oliver, W.C.; Pharr, G.M. An improved technique for determining hardness and elastic modulus using load and displacement sensing indentation experiments. *J. Mater. Res.* **1992**, *7*, 1564–1583. [[CrossRef](#)]
23. Vyazovkin, S. Modification of the integral isoconversional method to account for variation in the activation energy. *J. Comput. Chem.* **2001**, *22*, 178–183. [[CrossRef](#)]
24. Shi, X.; Nguyen, T.A.; Suo, Z.; Liu, Y.; Avci, R. Effect of nanoparticles on the anticorrosion and mechanical properties of epoxy coating. *Surf. Coat. Technol.* **2009**, *204*, 237–245. [[CrossRef](#)]
25. AlOtaibi, A.; Sherif, E.-S.M.; Zinelis, S.; Al-Jabbari, Y. Corrosion Behavior of Two cp Titanium Dental Implants Connected by Cobalt Chromium Metal Superstructure in Artificial Saliva and the Influence of Immersion Time. *Inter. J. Electrochem. Sci.* **2016**, *11*, 5877–5890. [[CrossRef](#)]
26. Seikh, A.H.; Halfa, H.; Sherif, E.-S.M. Corrosion resistance performance of newly developed cobalt-free maraging steel over conventional maraging steel in acidic media. *Adv. Mater. Proc. Technol.* **2016**, *2*, 283–292. [[CrossRef](#)]
27. Alharthi, N.; Sherif, E.-S.M.; Abdo, H.S.; El-Abedin, S.Z. Effect of nickel content on the corrosion resistance of iron-nickel alloys in concentrated hydrochloric acid pickling solutions. *Adv. Mater. Sci. Eng.* **2017**, *2017*. [[CrossRef](#)]
28. Gopi, D.; Sherif, E.-S.M.; Surendiran, M.; Sakila, D.M.A.; Kavitha, L. Corrosion inhibition by benzotriazole derivatives and sodium dodecyl sulphate as corrosion inhibitors for copper in ground water at different temperatures. *Surf. Interf. Anal.* **2015**, *47*, 618–625. [[CrossRef](#)]

29. Sherif, E.-S.M.; El-Danaf, E.A.; Abdo, H.S.; El-Abedin, S.Z.; Al-Khazraji, H. Effect of annealing temperature on the corrosion protection of hot swaged Ti-54M alloy in 2 M HCl pickling solutions. *Metals* **2017**, *7*, 29.
30. Sherif, E.-S.M.; Abdo, H.S.; El Abedin, S.Z. Electrochemical corrosion behavior of Fe64/Ni36 and Fe55/Ni45 alloys in 4.0% sodium chloride solutions. *Inter. J. Electrochem. Sci.* **2017**, *12*, 1600–1611. [[CrossRef](#)]
31. Tsai, P.Y.; Chen, T.E.; Lee, Y.L. Development and characterization of anticorrosion and antifriction properties for high performance polyurethane/graphene composite coatings. *Coatings* **2018**, *8*, 250. [[CrossRef](#)]
32. Akbarian, M.; Olya, M.E.; Mahdavian, M.; Ataefard, M. Effects of nanoparticulate silver on the corrosion protection performance of polyurethane coatings on mild steel in sodium chloride solution. *Prog. Org. Coat.* **2014**, *77*, 1233–1240. [[CrossRef](#)]



© 2019 by the authors. Licensee MDPI, Basel, Switzerland. This article is an open access article distributed under the terms and conditions of the Creative Commons Attribution (CC BY) license (<http://creativecommons.org/licenses/by/4.0/>).